

Overcoming the Limits of Vortex Formation in Magnetic Nanodots by Coupling to Antidot Matrix

R. V. Verba,^{1,2,*} D. Navas,¹ A. Hierro-Rodriguez,^{1,3} S. A. Bunyaev,¹ B. A. Ivanov,^{2,4}
K. Y. Guslienko,^{5,6} and G. N. Kakazei¹

¹*IFIMUP-IN/Departamento de Física e Astronomia, Universidade do Porto, 4169-007 Porto, Portugal*

²*Institute of Magnetism, Kyiv 03680, Ukraine*

³*SUPA, School for Physics and Astronomy, University of Glasgow, Glasgow G12 8QQ, United Kingdom*

⁴*National University of Science and Technology “MISiS,” Moscow 119049, Russian Federation*

⁵*Departamento de Física de Materiales, Universidad del País Vasco, UPV/EHU, 20018 San Sebastián, Spain*

⁶*IKERBASQUE, the Basque Foundation for Science, 48013 Bilbao, Spain*

(Received 15 May 2018; revised manuscript received 3 August 2018; published 17 September 2018)

Static magnetic configurations of thin, circular, soft (permalloy) magnetic nanodots, coupled to a hard antidot matrix with perpendicular magnetization, are studied by micromagnetic simulations. It is demonstrated that dipolar fields of the antidot matrix promote the formation of a magnetic-vortex state in nanodots. The vortex is the dot ground state at zero external field in ultrathin nanodots with diameters as low as 60 nm, which is far beyond the vortex stability range in an isolated permalloy nanodot. Depending on the geometry and antidot-matrix material, it is possible to stabilize either a radial vortex state or unconventional vortices with the angle between in-plane magnetization and radial direction $\psi \neq 0, \pi/2$.

DOI: 10.1103/PhysRevApplied.10.031002

Magnetic vortices are one of the simplest topologically nontrivial configurations that can be achieved in ferromagnetic films and nanostructures [1–3]. They have been extensively investigated during the past two decades, both from a fundamental point of view and in relation to applications in: magnetic recording [4–6]; microwaves, including magnonic crystals [7,8] and high-power vortex spin-torque oscillators [9–11]; medicine [12]; etc. For several applications, it is desirable to stabilize the magnetic vortex in a nanodot with the smallest possible thickness and lateral dimensions. For example, spin-transfer torque efficiency in magnetic-tunnel-junction-based spin-torque oscillators is inversely proportional to the thickness [10]; usage of interface effects like voltage-controlled magnetic anisotropy [13,14], the spin Hall effect [15,16], and interfacial Dzyaloshinskii-Moriya interaction [17,18], which may increase the functionality and efficiency of vortex-based devices, also requires thickness less than 5 nm. A decrease of lateral sizes results in higher frequencies of vortex excitations [2] and allows us to enhance integrability.

However, in the simplest and the most studied geometry—a thin circular nanodot, made of soft magnetic material—the vortex state can be realized only in relatively large dots, while smaller ones exist in a quasiuniform single-domain state. The minimal dot diameter required to

make the vortex state the ground one (a state corresponding to the global magnetic energy minimum) at zero external field inversely depends on the dot thickness [19,20]. For example, for commonly used soft ferromagnetic permalloy ($\text{Ni}_{80}\text{Fe}_{20}$) of thickness $t_d = 10$ nm, the minimal diameter is about $d_d = 80$ nm; for $t_d = 5$ nm, it is 160 nm [19]. However, metastability of the quasiuniform state in a large area close to the geometrical parameters, at which the vortex state becomes the ground state [20], complicates the observation and usage of vortices in this range, since it is impossible to nucleate a vortex by a bias field decrease from in-plane or out-of-plane saturation. To guarantee vortex appearance, the single-domain state should become unstable in zero field. This case is realized if the dot thickness is larger than $t_d \gtrsim 30\pi\lambda_{\text{ex}}^2/d_d$ [20], where λ_{ex} is the material exchange length ($\lambda_{\text{ex}} \approx 5.5$ nm for permalloy), i.e., $t_d > 14$ nm for a 200-nm diameter and $t_d > 28$ nm for $d_d = 100$ nm. For this reason, almost all of the experiments are performed for the dot thickness $t_d > 10$ nm [21]. An exception is vortex spin-torque oscillators, in which an Oersted field of bias current promotes the vortex formation and solves the problem with a metastable quasiuniform state, making possible the operation with 5–10-nm-thick free layers [9–11].

In this paper, we show how to achieve a vortex ground state in much smaller nanodots with ultrathin thickness and diameters down to 50 nm and how to switch a dot into a vortex state in the region, where it is metastable. Our

*verrv@ukr.net

approach is based on the dipolar coupling of a soft magnetic nanodot with a perpendicularly magnetized antidot matrix, dipolar stray fields of which have the necessary radial symmetry and promote vortex formation.

There are different types of magnetic vortices. In general, a two-dimensional vortex is the topologically non-trivial magnetization configuration with winding number $v = 1$ [22]. Magnetization distribution away from the vortex core is determined by $\phi = \chi + \psi$, where ϕ is the azimuthal angle of magnetization (i.e., $M_x/M_s = \cos \phi$, $M_y/M_s = \sin \phi$), χ is the azimuthal coordinate in a polar coordinate system, and ψ is the parameter determining vortex structure. In most cases, vortices with $\psi = \pm\pi/2$, which have a closure-flux structure, have been studied. Properties of such vortices have been investigated in: easy-plane anisotropic films [1]; thin circular nanodots, including static properties [19,20,23], linear (see Ref. [2] and references therein) and nonlinear [24–26] dynamics; nanodot arrays [7,27]; relatively thick nanodots [28,29]; stacked two-dot systems [30]; and other more complex geometries. Vortices with other values of ψ are often called “unconventional vortices” [31]. For $\psi = 0, \pi$ these are “radial vortices,” which have been observed in ultrathin nanodots with interfacial Dzyaloshinskii-Moriya interaction [32], in pairs of nanodots with antiferromagnetic exchange coupling [33,34], and at the crosses of ferromagnetic nanowires [31]. Vortices with $\psi \neq 0, \pm\pi/2, \pi$ have been realized in thick circular nanodots (however, their structure is thickness dependent) [29,31]. Interestingly, these unconventional vortices have been proposed as a pinned layer in skyrmion-based spin-torque oscillators and revealed characteristics that cannot be achieved by using common vortices [35].

The patterned film under consideration is shown in Fig. 1. It is a layer of hard magnetic material with perpendicular magnetization of thickness t_{HL} , having an antidot of diameter d_{ad} . Inside an antidot, there is a nanodot of thickness t_d and diameter d_d , made of soft magnetic material. The dot is grown on the same substrate as the hard magnetic layer, resulting in an asymmetric vertical position of the dot respective to the hard layer. We assume that the direct exchange coupling between the dot and hard layer is absent; that is the case, e.g., if the dot diameter is smaller than the antidot diameter, as shown in Fig. 1(a). In subsequent calculations, we use a 10-nm difference between diameters of the antidot and dot.

The magnetization distribution in the nanostructure is studied using a MuMax3 micromagnetic solver [36]. As a dot material, we choose permalloy (saturation magnetization $M_s = 8.1 \times 10^5$ A/m, exchange stiffness $A = 1.05 \times 10^{-11}$ J/m); the parameters of the hard magnetic layer are set as $M_s = 10^6$ A/m, $A = 2 \times 10^{-11}$ J/m, and the constant of uniaxial perpendicular anisotropy $K_u = 7 \times 10^5$ J/m³, which correspond to FePd, FePt, and CoPt multilayers of different composition. Strictly speaking, the

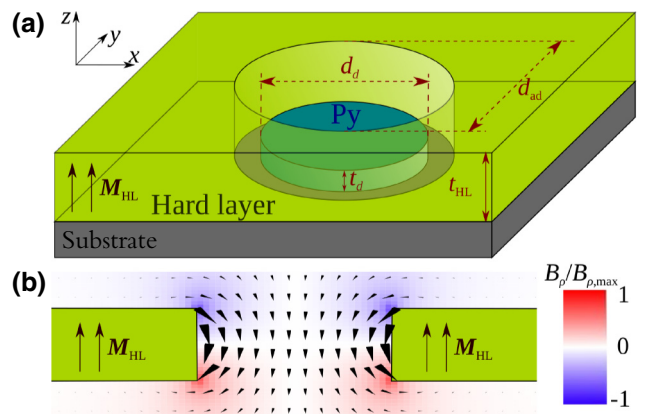


FIG. 1. (a) A sketch of the considered nanostructure—a soft magnetic nanodot placed within an antidot in a hard magnetic layer with perpendicular magnetization. (b) Distribution of stray fields in the antidot; arrow length corresponds to the field magnitude and color to the field radial component B_ρ .

only important characteristic of the hard layer for the studied case is M_s , while anisotropy should simply be strong enough to guarantee a stable perpendicular magnetization state in zero field. The minimal required anisotropy, in a general case, depends on the antidot lattice geometry [37,38]. Our simulations confirm a stable quasuniform OOP magnetization in zero field (after perpendicular saturation) in the whole studied range for the chosen material parameters. Notes on different hard layer magnetizations, as well as on different locations of a dot, are given later. The cell size is chosen to be $2.5 \times 2.5 \times 1.5$ nm³ or $1.25 \times 1.25 \times 1$ nm³ for the smallest dots. To avoid edge effects, we set periodic boundary conditions with period 400 nm, which is large enough not to produce interdot interaction.

The perpendicularly magnetized hard layer creates magnetostatic stray fields inside the antidot and in its vicinity. The stray fields are radially symmetric and have radial B_ρ and perpendicular B_z components [Fig. 1(b)]. The radial component is zero at the central plane and reaches a maximum close to the top and bottom hard layer surfaces.

Firstly, we consider the effect of the hard layer thickness, fixing the dot thickness to $t_d = 3$ nm and investigating the dot remanent states that appear after perpendicular saturation by the external field $\vec{B} = B_z \vec{e}_z$ and then the gradual decrease of the field to zero. In the case $t_{HL} = t_d$, the radial component of stray fields averaged over the dot thickness is zero, and we observe a quasuniform single-domain “leaflike” state [Fig. 3(a)] in the entire simulation range (Fig. 2). It is expected, as for an isolated dot of the thickness $t_d = 3$ nm, the single-domain state is the ground one up to approximately a 235-nm dot diameter and remains stable up to a 1-μm dot diameter. Therefore, the vortex nucleation in an isolated dot of such thickness is almost impossible.

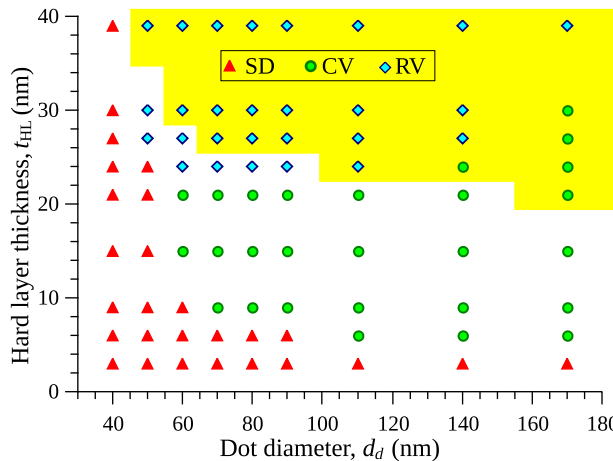


FIG. 2. Diagram of the magnetization remanent states of a nanodot of thickness $t_d = 3$ nm. SD denotes a single-domain state, CV a curled vortex, and RV a radial vortex. The yellow area shows the region where the vortex state is the ground state.

However, as soon as t_{HL} increases, the radial component of the stray field becomes nonzero and we start to observe a vortex state at remanence. With an increase of the hard layer thickness, the vortex state becomes more and more favorable and, for $t_{\text{HL}} = 39$ nm, we observe it even for a 50-nm nanodot diameter (Fig. 2).

Note that, in all of the cases, the remanent state is an “unconventional” vortex. For a strong enough stray field emanated by the matrix (large matrix thickness), the Zeeman energy of the dot magnetization in the stray field dominates and a radial vortex is formed [Fig. 3(c)]. The radial vortex has a small core region with out-of-plane magnetization and an in-plane magnetization part, divergent ($\psi = 0$) or convergent ($\psi = \pi$) to the center. The direction of the in-plane part depends, naturally, on the magnetization of the matrix. In our case, $M_{z,\text{HL}}/M_s = +1$, the matrix creates a divergent radial field at the bottom, resulting in divergent magnetization of the vortex. If one reverses the matrix magnetization or places the dot at the top of the matrix, the vortex structure will be convergent.

With a decrease of the hard layer thickness and/or an increase of the dot diameter, the demagnetization energy becomes more important and it competes with Zeeman energy, resulting in the formation of a curled unconventional vortex. It is characterized by $\psi \neq 0, \pm\pi/2, \pi$, which, strictly speaking, depends on the distance from the dot center $\psi = \psi(\rho)$ [see the example in Fig. 3(b)]. The value of ψ changes gradually with geometrical parameters; in particular, in the limit $d_d \gg t_{\text{HL}}$, the vortex structure is transformed to a conventional vortex with $\psi = \pm\pi/2$. Thus, the proposed approach gives the ability to tune the vortex structure and achieve unconventional vortices with a given ψ that can be necessary, e.g., for skyrmion-based spin-torque oscillators [35]. It should also be noted that, in both cases of radial and curled vortices, their out-of-core regions have a small perpendicular component due to the influence of the perpendicular stray field of the antidot matrix. This component disappears at a certain nonzero external field $B_z \neq 0$.

We check if the vortex state is the ground one by a comparison of its energy in zero field with the energy of a single-domain state, which is manually introduced and allowed to relax into a local energy minimum. The corresponding region of the vortex ground state is smaller than the region where the vortex state is achieved at remanence (Fig. 2). However, a sufficiently thick matrix allows us to make the vortex configuration the ground state in dots with diameters well below 100 nm. For practical applications, it is desirable, of course, to work in this vortex-ground-state region. However, outside of this region, a vortex can also be nucleated in practice by the decrease of the external field from perpendicular saturation, as has been done in simulations. It happens because stray fields of the antidot promote the formation of radial vortex, which then may transform into a curled vortex, when B_z is gradually decreased. Because of the energy barriers between the vortex and saturated states [39,40], the vortex state remains stable at remanence. Only in the region where the vortex state is unstable with respect to small perturbations, one cannot observe vortex (the single-domain region in Fig. 2). It is in contrast to the case of an isolated dot,

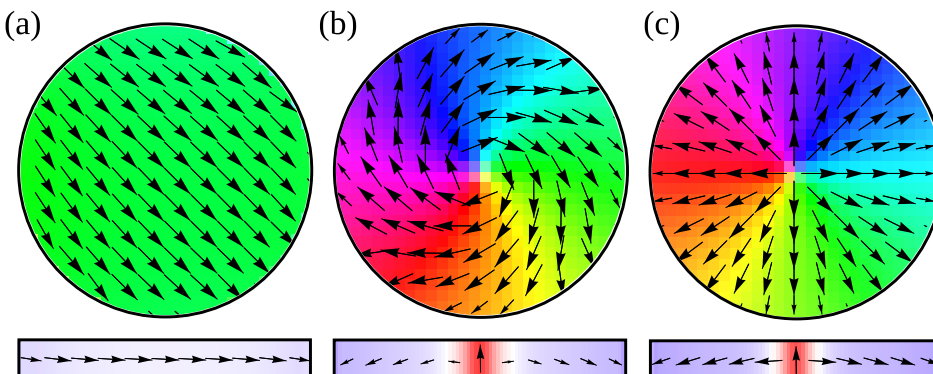


FIG. 3. Magnetization configuration of the 70-nm-diameter dot in a (a) single-domain state (hard layer thickness $t_{\text{HL}} = 6$ nm), (b) curled vortex state ($t_{\text{HL}} = 15$ nm), and (c) radial vortex state ($t_{\text{HL}} = 24$ nm). Top: Top view. Bottom: y - z cross section. The dot thickness $t_d = 3$ nm.

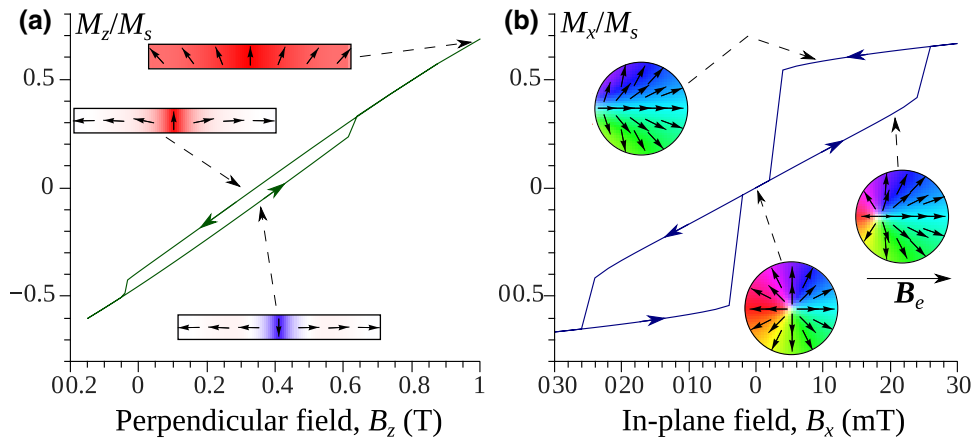


FIG. 4. Out-of-plane (a) and in-plane (b) hysteresis loops of a nanodot in the vortex ground state and corresponding magnetization distributions. The dot diameter $d_d = 90$ nm, dot thickness $t_d = 3$ nm, and hard layer thickness $t_{HL} = 30$ nm. In the plots, only the magnetization of the dot is accounted for.

where a uniform bias field does not help the vortex formation and the single-domain state remains at zero field in the metastability range.

As in the case of a common vortex [41], the core polarity of unconventional vortices can be switched by a perpendicular external magnetic field. The corresponding hysteresis loop is, of course, shifted with respect to zero field [Fig. 4(a)] due to the influence of perpendicular component of the antidot stray field. This shift is more pronounced for thicker matrices and, for a sufficiently thick matrix, both switching fields can be positive, meaning that only the state with the core polarity opposite to the matrix magnetization remains stable at zero bias field.

The behavior of unconventional vortices in an in-plane bias field is also similar to that for a common vortex [23]. The corresponding hysteresis loop has a characteristic “double-triangle” shape; the vortex is expelled from the dot at an annihilation field and nucleates when the field decreases to a nucleation field [Fig. 4(b)]. Naturally, the core polarity of a nucleated vortex is opposite to that of the matrix magnetization, as it is energy favorable. Under an in-plane applied field, the core of the radial vortex moves opposite to the field direction [see the insets in Fig. 4(b)], while the core of the curled vortex moves at some finite angle ($\neq \pi/2$) to the field direction. In contrast, the core of the common vortex moves perpendicularly to the field [23]. This different behavior is a consequence of different distributions of the in-plane part of vortex magnetization. Thus, one can nucleate and manipulate vortices in the considered nanoscale dots with relatively small in-plane magnetic fields (of course, if the matrix is magnetized perpendicularly before). However, this method works only in the region of a vortex ground state. Outside of it, the vortex does not nucleate after in-plane saturation of the nanodot.

Next, we investigate the role of the permalloy dot thicknesses t_d . To do this, we fix the hard layer thickness to

$t_{HL} = 24$ nm and perform simulations for different values of t_d . As one can see from the states diagram (Fig. 5), vortex become the ground state in dots with smaller diameters when the dot thickness is decreased. This tendency is opposite to that for an isolated dot. Also, for thinner dots, the formation of radial vortices becomes more favorable. These features are related to the reduction of demagnetization energy of the radial vortex state with a decrease of the thickness-to-diameter aspect ratio of the dot.

As is clear from the previous consideration, the main impact of the antidot matrix is the radial component of stray fields, which it creates. Within the antidot matrix, at the top or bottom of the hard layer, this component is approximately equal to

$$B_\rho \approx \pm \mu_0 M_{s,HL} \frac{\rho}{2d_{ad}} \left(1 - \left[1 + \frac{2t_{HL}}{d_{ad}} \right]^{-3/2} \right), \quad (1)$$

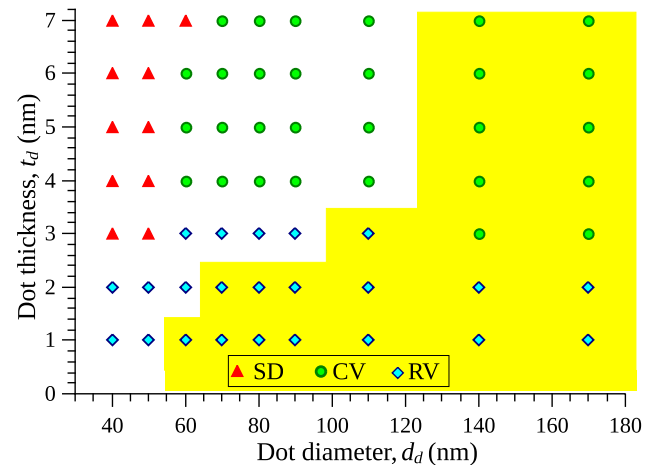


FIG. 5. Diagram of the magnetization remanent states of a nanodot in an antidot matrix of thickness $t_{HL} = 24$ nm. Notation is the same as in Fig. 2.

where ρ is the distance from the antidot center (this estimation assumes $t_d \ll t_{\text{HL}}$ and is valid for $\rho < d_{\text{ad}}/2$, except for the region close to the antidot edge). B_ρ is proportional to the saturation magnetization of the hard layer and to its thickness (up to $t_{\text{HL}} \gg d_{\text{ad}}$, where it saturates). Thus, one may reduce the hard layer thickness by using materials with higher M_s or use materials with lower M_s and sufficiently large thickness. The behavior of the dot is the same if B_ρ is fixed. Also, it is clear that one can place the dot in another way than what is shown in Fig. 1(a). For example, a dot of smaller, equal, or slightly larger diameter than the antidot can be placed on top of the antidot matrix. The only requirements are the presence of radial stray fields and the absence of an exchange coupling between the dot and the matrix, which may drastically affect the magnetization distribution in a dot.

In conclusion, we have demonstrated that dipolar coupling with a perpendicularly magnetized antidot matrix can substantially enlarge the region of vortex stability in soft magnetic circular nanodots to the range of ultrathin thicknesses and sub-100-nm diameters. The main impact is produced by the radial component of the antidot stray field, which leads to the appearance and stabilization of the magnetic vortices with unconventional textures. The vortex magnetization configuration can be tuned by a proper choice of geometrical parameters of the patterned film. In the case of a sufficiently thick matrix and thin dots, the radial vortices are formed, and unconventional curled vortices with an angle between the in-plane magnetization and radial direction $\psi \neq 0, \pm\pi/2, \pi$ are stabilized otherwise. The vortices can be nucleated by the magnetic-field decrease, starting from a perpendicular saturated state and, except for the range of vortex metastability, starting from an in-plane saturated state, provided that the antidot matrix is in a perpendicular single-domain state.

The application of proposed nanostructures could significantly improve the characteristics of vortex-based spintronic devices, e.g., vortex spin-torque oscillators. Indeed, thinner free layers, 2–3 nm in thickness, allow us to reduce the bias-current density up to 3–5 times compared to commonly used isolated vortex-state dots with 10–20-nm thickness. Small dot diameters, together with the presence of an additional restoring force coming from the matrix stray field, result in a higher frequency of the gyrotropic mode of the vortex. For example, in preliminary simulations, for 3-nm dot thickness and $t_{\text{HL}} = 39$ nm, we observe a gyrotropic-mode frequency as high as 1–1.5 GHz. Such frequencies can be accessed in isolated dots of the thickness about 50 nm [29,42], which are incompatible with spin-transfer-torque-based devices. Of course, the detailed study of dynamic properties of the nanostructure is a topic for a separate work. Finally, the stabilization of unconventional vortices is important for skyrmion-based spin-torque oscillators [35].

ACKNOWLEDGMENTS

The Portuguese team acknowledges the Network of Extreme Conditions Laboratories-NECL and Portuguese Foundation of Science and Technology (FCT) support through the projects NORTE-01-0145-FEDER-022096, MIT-EXPL/IRA/0012/2017, POCI-0145-FEDER-030085 (NOVAMAG), EXPL/IF/01191/2013 (D.N.), EXPL/IF/00541/2015 (S.A.B.), EXPL/IF/00981/2013 (G.N.K.), and SFRH/BPD/90471/2012 (A.H.-R.). This work was also supported by the Ministry of Education and Science of Ukraine, project No. 0118U004007 (R.V.V., B.A.I.); IKERBASQUE (the Basque Foundation for Science) (K.Y.G.); the Spanish MINECO, Grants No. FIS2016-78591-C3-3-R (K.Y.G.) and No. FIS2016-76058-C4-4-R (A.H.-R.); the European Union Horizon 2020 Research and Innovation Programme under Marie Skłodowska-Curie Grants No. 644348 (R.V.V., B.A.I., K.Y.G.) and No. H2020-MSCA-IF-2016-746958 (A.H.-R.). B.A.I. was supported by the Program of NUST “MISiS” (Grant No. K2-2017-005), implemented by a governmental decree No. 211 dated March 16, 2013. G.N.K. acknowledges the support from European Cooperation in Science and Technology (COST) project CA16218 “NANOCOHYBRI.”

- [1] D. L. Huber, Dynamics of spin vortices in two-dimensional planar magnets, *Phys. Rev. B* **26**, 3758 (1982).
- [2] K. Yu. Guslienko, Magnetic vortex state stability, reversal and dynamics in restricted geometries, *J. Nanosci. Nanotechnol.* **8**, 2745 (2008).
- [3] R. Antos, Y. Otani, and J. Shibata, Magnetic vortex dynamics, *J. Phys. Soc. Japan* **77**, 031004 (2008).
- [4] B. VanWaeyenberge, A. Puzic, H. Stoll, K. W. Chou, T. Tyliaszczak, R. Hertel, M. Fahnle, H. Bruckl, K. Rott, G. Reiss, I. Neudecker, D. Weiss, C. H. Back, and G. Schutz, Magnetic vortex core reversal by excitation with short bursts of an alternating field, *Nature* **444**, 461 (2006).
- [5] R. Hertel, S. Gliga, M. Fähnle, and C. M. Schneider, Ultrafast nanomagnetic toggle switching of vortex cores, *Phys. Rev. Lett.* **98**, 117201 (2007).
- [6] M. Kammerer, M. Weigand, M. Curcic, M. Noske, M. Sproll, A. Vansteenkiste, B. Van Waeyenberge, H. Stoll, G. Woltersdorf, C. H. Back, and G. Schuetz, Magnetic vortex core reversal by excitation of spin waves, *Nat. Commun.* **2**, 279 (2011).
- [7] A. A. Awad, K. Y. Guslienko, J. F. Sierra, G. N. Kakazei, V. Metlushko, and F. G. Aliev, Spin excitation frequencies in magnetostatically coupled arrays of vortex state circular Permalloy dots, *Appl. Phys. Lett.* **96**, 012503 (2010).
- [8] D.-S. Han, A. Vogel, H. Jung, K.-S. Lee, M. Weigand, H. Stoll, G. Schütz, P. Fischer, G. Meier, and S.-K. Kim, Wavemodes of collective vortex gyration in dipolar-coupled-dot-array magnonic crystals, *Sci. Rep.* **3**, 2262 (2013).

- [9] R. Lehndorff, D. E. Bürgler, S. Gliga, R. Hertel, P. Grünberg, C. M. Schneider, and Z. Celinski, Magnetization dynamics in spin torque nano-oscillators: Vortex state versus uniform state, *Phys. Rev. B* **80**, 054412 (2009).
- [10] A. Dussaux, B. Georges, J. Grollier, V. Cros, A. V. Khvalkovskiy, A. Fukushima, M. Konoto, H. Kubota, K. Yakushiji, S. Yuasa, K. A. Zvezdin, K. Ando, and A. Fert, Large microwave generation from current-driven magnetic vortex oscillators in magnetic tunnel junctions, *Nat. Commun.* **1**, 8 (2010).
- [11] S. Tsunegi, H. Kubota, K. Yakushiji, M. Konoto, S. Tamaru, A. Fukushima, H. Arai, H. Imamura, E. Grimaldi, R. Lebrun, J. Grollier, V. Cros, Shinji Yuasa, High emission power and Q factor in spin torque vortex oscillator consisting of FeB free layer, *Appl. Phys. Express* **7**, 063009 (2014).
- [12] D.-H. Kim, E. A. Rozhkova, I. V. Ulasov, S. D. Bader, T. Rajh, M. S. Lesniak, and V. Novosad, Biofunctionalized magnetic-vortex microdisks for targeted cancer-cell destruction, *Nat. Mater.* **9**, 165 (2010).
- [13] M. Weisheit, S. Fähler, A. Marty, Y. Souche, C. Poinsignon, and D. Givord, Electric field-induced modification of magnetism in thin-film ferromagnets, *Science* **315**, 349 (2007).
- [14] C.-G. Duan, J. P. Velev, R. F. Sabirianov, Z. Zhu, J. Chu, S. S. Jaswal, and E. Y. Tsymbal, Surface magnetoelectric effect in ferromagnetic metal films, *Phys. Rev. Lett.* **101**, 137201 (2008).
- [15] K. Ando, S. Takahashi, K. Harii, K. Sasage, J. Ieda, S. Maekawa, and E. Saitoh, Electric manipulation of spin relaxation using the spin Hall effect, *Phys. Rev. Lett.* **101**, 036601 (2008).
- [16] V. E. Demidov, S. Urazhdin, H. Ulrichs, V. Tiberkevich, A. Slavin, D. Bather, G. Schmitz, and S. O. Demokritov, Magnetic nano-oscillator driven by pure spin current, *Nat. Mater.* **11**, 1028 (2011).
- [17] M. Bode, M. Heide, K. von Bergmann, P. Ferriani, S. Heinze, G. Bihlmayer, A. Kubetzka, O. Pietzsch, S. Blügel, and R. Wiesendanger, Chiral magnetic order at surfaces driven by inversion asymmetry, *Nature* **447**, 190 (2007).
- [18] L. Uvdvardi and L. Szunyogh, Chiral asymmetry of the spin-wave spectra in ultrathin magnetic films, *Phys. Rev. Lett.* **102**, 207204 (2009).
- [19] K. L. Metlov and K. Yu. Guslienko, Stability of magnetic vortex in soft magnetic nano-sized circular cylinder, *J. Magn. Magn. Matter.* **242**, 1015 (2002).
- [20] K. L. Metlov and Y. P. Lee, Map of metastable states for thin circular magnetic nanocylinders, *Appl. Phys. Lett.* **92**, 112506 (2008).
- [21] S.-H. Chung, R. D. McMichael, D. T. Pierce, and J. Unguris, Phase diagram of magnetic nanodisks measured by scanning electron microscopy with polarization analysis, *Phys. Rev. B* **81**, 024410 (2010).
- [22] N. D. Mermin, The topological theory of defects in ordered media, *Rev. Mod. Phys.* **51**, 591 (1979).
- [23] K. Yu. Guslienko, V. Novosad, Y. Otani, H. Shima, and K. Fukamichi, Magnetization reversal due to vortex nucleation, displacement, and annihilation in submicron ferromagnetic dot arrays, *Phys. Rev. B* **65**, 024414 (2001).
- [24] K. S. Buchanan, M. Grimsditch, F. Y. Fradin, S. D. Bader, and V. Novosad, Driven dynamic mode splitting of the magnetic vortex translational resonance, *Phys. Rev. Lett.* **99**, 267201 (2007).
- [25] O. V. Sukhostavets, B. Pigeau, S. Sangiao, G. de Loubens, V. V. Naletov, O. Klein, K. Mitsuzuka, S. Andrieu, F. Montaigne, and K. Y. Guslienko, Probing the anharmonicity of the potential well for a magnetic vortex core in a nanodot, *Phys. Rev. Lett.* **111**, 247601 (2013).
- [26] E. Holmgren, A. Bondarenko, M. Persson, B. A. Ivanov, and V. Korenivski, Transient dynamics of strongly coupled spin vortex pairs: Effects of anharmonicity and resonant excitation on inertial switching, *Appl. Phys. Lett.* **112**, 192405 (2018).
- [27] V. Novosad, K. Yu. Guslienko, H. Shima, Y. Otani, S. G. Kim, K. Fukamichi, N. Kikuchi, O. Kitakami, and Y. Shimada, Effect of interdot magnetostatic interaction on magnetization reversal in circular dot arrays, *Phys. Rev. B* **65**, 060402 (2002).
- [28] K. Y. Guslienko, G. N. Kakazei, J. Ding, X. M. Liu, and A. O. Adeyeye, Giant moving vortex mass in thick magnetic nanodots, *Sci. Rep.* **5**, 13881 (2015).
- [29] R. V. Verba, A. Hierro-Rodriguez, D. Navas, J. Ding, X. M. Liu, A. O. Adeyeye, K. Y. Guslienko, and G. N. Kakazei, Spin-wave excitation modes in thick vortex-state circular ferromagnetic nanodots, *Phys. Rev. B* **93**, 214437 (2016).
- [30] S. S. Cherepov, B. C. Koop, A. Yu. Galkin, R. S. Khymyn, B. A. Ivanov, D. C. Worledge, and V. Korenivski, Core-core dynamics in spin vortex pairs, *Phys. Rev. Lett.* **109**, 097204 (2012).
- [31] M. Yan, H. Wang, and C. E. Campbell, Unconventional magnetic vortex structures observed in micromagnetic simulations, *J. Magn. Magn. Mater.* **320**, 1937 (2008).
- [32] G. Siracusano, R. Tomasello, A. Giordano, V. Puliafito, B. Azzerboni, O. Ozatay, M. Carpentieri, and G. Finocchio, Magnetic radial vortex stabilization and efficient manipulation driven by the Dzyaloshinskii-Moriya interaction and spin-transfer torque, *Phys. Rev. Lett.* **117**, 087204 (2016).
- [33] C. Phatak, A. K. Petford-Long, and O. Heinonen, Direct observation of unconventional topological spin structure in coupled magnetic discs, *Phys. Rev. Lett.* **108**, 067205 (2012).
- [34] S. Wintz, C. Bunce, A. Neudert, M. Körner, T. Strache, M. Buhl, A. Erbe, S. Gemming, J. Raabe, C. Quitmann, and J. Fassbender, Topology and origin of effective spin meron pairs in ferromagnetic multilayer elements, *Phys. Rev. Lett.* **110**, 177201 (2013).
- [35] F. Garcia-Sanchez, J. Sampaio, N. Reyren, V. Cros, and J.-V. Kim, A skyrmion-based spin-torque-nano-oscillator, *New J. Phys.* **18**, 075011 (2016).
- [36] A. Vansteenkiste, J. Leliaert, M. Dvornik, M. Helsen, F. Garcia-Sanchez, and B. Van Waeyenberge, The design and verification of MuMax3, *AIP Adv.* **4**, 107133 (2014).
- [37] J. Gräfe, M. Weigand, N. Träger, G. Schütz, E. J. Goering, M. Skripnik, U. Nowak, F. Haering, P. Ziemann, and U. Wiedwald, Geometric control of the magnetization reversal in antidot lattices with perpendicular magnetic anisotropy, *Phys. Rev. B* **93**, 104421 (2016).
- [38] M. Krupinski, D. Mitin, A. Zarzycki, A. Szkudlarek, M. Giersig, M. Albrecht, and M. Marszaek, Magnetic transition from dot to antidot regime in large area Co/Pd

- nanopatterned arrays with perpendicular magnetization, *Nanotechnology* **28**, 085302 (2017).
- [39] G. N. Kakazei, M. Ilyn, O. Chubykalo-Fesenko, J. Gonzalez, A. A. Serga, A. V. Chumak, P. A. Beck, B. Laegel, B. Hillebrands, and K. Y. Guslienko, Slow magnetization dynamics and energy barriers near vortex state nucleation in circular permalloy dots, *Appl. Phys. Lett.* **99**, 052512 (2011).
- [40] G. A. Melkov, Y. Kobljanskyj, V. Novosad, A. N. Slavin, and K. Y. Guslienko, Probing the energy barriers in nonuniform magnetization states of circular dots by broadband ferromagnetic resonance, *Phys. Rev. B* **88**, 220407 (2013).
- [41] G. de Loubens, A. Riegler, B. Pigeau, F. Lochner, F. Boust, K. Y. Guslienko, H. Hurdequint, L. W. Molenkamp, G. Schmidt, A. N. Slavin, V. S. Tiberkevich, N. Vukadinovic, and O. Klein, Bistability of vortex core dynamics in a single perpendicularly magnetized nanodisk, *Phys. Rev. Lett.* **102**, 177602 (2009).
- [42] J. Ding, G. N. Kakazei, X. Liu, K. Y. Guslienko, and A. O. Adeyeye, Higher order vortex gyrotropic modes in circular ferromagnetic nanodots, *Sci. Rep.* **4**, 4796 (2014).